Thermal Hall effect of spins in a paramagnet

Hyunyong Lee, Jung Hoon Han, and Patrick A. Lee

Phys. Rev. B **91**, 125413 — Published 10 March 2015

DOI: 10.1103/PhysRevB.91.125413

Thermal Hall Effect of Spins in a Paramagnet

Hyunyong Lee,[1] Jung Hoon Han,[1,*] and Patrick A. Lee[2,†]

[1]*Department of Physics, Sungkyunkwan University, Suwon 440-746, Korea*
[2]*Department of Physics, Massachusetts Institute of Technology, Cambridge, Massachusetts 02139, USA*

Theory of Hall transport of spins in a correlated paramagnetic phase is developed. By identifying the thermal Hall current operator in the spin language, which turns out to equal the spin chirality in the pure Heisenberg model, various response functions can be derived straightforwardly. Subsequent reduction to the Schwinger boson representation of spins allows a convenient calculation of thermal and spin Hall coefficients in the paramagnetic regime using self-consistent mean-field theory. Comparison is made to results from the Holstein-Primakoff reduction of spin operators appropriate for ordered phases.

I. INTRODUCTION

The Hall effect of electrons has evolved from a useful tool for measuring the carrier density of a material to a powerful diagnostic of the topological structure of the underlying electronic band, reflecting the Berry curvature distribution throughout the Brillouin zone [1,2]. Hall effect of charge current often implies the Hall effect for the energy, or of thermal transport, as the motion of electrons necessarily involves the transport of energy as well.

Exciting recent developments have been the realization that this notion of topology-driven Hall effect can be extended to neutral objects of zero electrical charge. Phonon Hall effect, in which a transverse heat transport is mediated by phonons in response to thermal gradient, has been observed [3]. Magnons - quantized small fluctuations of an ordered magnet - can in principle exhibit similar Hall transport driven by thermal gradient, as first predicted theoretically by Katsura, Nagaosa, and Lee [4] and confirmed experimentally in an insulating pyrochlore magnet $Lu_2V_2O_7$ by the Tokura group [5]. Formulation of the magnon Hall effect was perfected by Murakami and collaborators in a series of papers [6–8] after correcting for the missing, magnetization current term in the original derivation of Ref. 4. A striking parallel of the topology of the magnon band structure to that of electronic bands responsible for quantized Hall effect was emphasized in several recent papers [9,10].

With a solid theoretical foundation and an experimental demonstration to back it up, the thermal Hall effect has become a powerful probe of the topological nature of magnon excitations in an ordered magnet. While the magnon Hall effect is easily interpreted as a natural consequence of momentum-space topology of the magnon band, a complementary real-space picture suggests that it is also a probe of a particular type of spin correlations, known as the spin chirality, of quantum insulating magnetic systems [4,5]. Spin chirality, expressed as the triple product of three neighboring spin operators $\mathbf{S}_i \cdot \mathbf{S}_j \times \mathbf{S}_k$ for sites i, j, k forming the smallest triangle in the lattice, has taken on the significance of an important new order parameter of a quantum spin system since its invention in the late 80's [11,12]. An appealing possibility entertained ever since its inception is that of a quantum-disordered magnet with zero average local magnetization $\langle \mathbf{S}_i \rangle = 0$ yet with a finite spin chirality, $\langle \mathbf{S}_i \cdot \mathbf{S}_j \times \mathbf{S}_k \rangle \neq 0$. Such a state breaks time-reversal symmetry and parity, opening the door for finite Hall-type transport in its ground state. A well-deserving question in this regard is whether the magnon Hall effect has a natural extension to the disordered phase, in which the notion of magnon may break down but not that of the spin chirality order. In other words, is the establishment of spin chirality (without the magnetic long-range order) a sufficient condition to give rise to thermal Hall effect in an insulating magnet?

We will argue in this paper that there is no physical principle preventing the persistence of Hall-type transport into the paramagnetic phases of spin once the time reversal symmetry is broken by the magnetic field. Thermal Hall measurement was successfully carried out both below and *above the ferromagnetic transition temperature* in a different material by the Ong group. [13] Recently the same group shows the presence of thermal Hall effect in the frustrated (i.e. disordered) quantum pyrochlore material $Tb_2Ti_2O_7$. [14] Stimulated by their observations, we go beyond the existing magnon description of the thermal Hall effect [4–10] and formulate the phenomenon using the spin language entirely. It is then applied to discuss Hall effects of spin both in the paramgnetic as well as the ferromagnetic regime. Essentially, the idea is to develop the linear response formalisms within the spin language as much as possible. Only in the final stage of the computation of the response function is the particular representation of the spin operator relevant. For instance the Hall effect in the ordered phase is appropriately captured by the Holstein-Primakoff (HP) mapping of spins, as had been done in the past, [4] while the possible paramagnetic Hall effect is best discussed in the Schwinger boson (SB) language. [15,16] Both thermal and spin Hall effects can be consistently described in this new formalism.

In Sec. II we describe the new linear response formalism for calculating thermal Hall conductivity entirely in the spin language, followed in Sec. III by an explicit calculation of the thermal and (related) spin Hall conductivities using the two well-known approximate methods: Holstein-Primakoff and Schwinger boson methods. Discussions and future prospects are given in Sec. IV.

II. SPIN LINEAR RESPONSE THEORY

To present the method of approach in a concrete background we choose the Heisenberg spin model on a Kagome lattice, written as a sum of site Hamiltonians $H = \sum_i H_i$, where each H_i is

$$H_i = \frac{1}{2}\sum_{j\in i}\Big(-J\mathbf{S}_i\cdot\mathbf{S}_j + D_{i;j}\mathbf{S}_i\times\mathbf{S}_j\cdot\hat{z}\Big) - B\mathbf{S}_i\cdot\hat{b}. \quad (1)$$

The symbol $j \in i$ indicates four immediate neighbors of each site i. The orientation of the external field is fixed: $\hat{b} = +\hat{z}$. Nearest-neighbor exchange interaction of strength J is assumed, with the convention for the sign of the Dzyaloshinskii-Moriya (DM) interaction $D_{i;j} = D = -D_{j;i}$ as outlined in Fig. 1. Although all formal derivations of spin linear response functions apply for either signs of J, for concreteness we will assume ferromagnetic exchange $J > 0$.

Two continuity equations are derived,

$$\dot{S}_i^z + \sum_{j\in i} J_{i;j}^S = 0, \quad \dot{H}_i + \sum_{j\in i} J_{i;j}^E = 0, \quad (2)$$

tied to total z-spin and energy conservations, respectively. The bond current operators are

$$\begin{aligned}
J_{i;j}^S &= -i\frac{J'}{2}e^{i\phi_{i;j}}S_i^+S_j^- + h.c.,\\
J_{i;j}^E &= -BJ_{i;j}^S - \frac{1}{2}\sum_{k\in j}\Big(JS_k^zJ_{i;j}^S + JS_i^zJ_{j;k}^S + [J_{i;j}^S,\, J_{j;k}^S]\Big)\\
&\quad + \frac{1}{2}\sum_{k\in i}\Big(JS_k^zJ_{j;i}^S + JS_j^zJ_{i;k}^S + [J_{j;i}^S,\, J_{i;k}^S]\Big). \quad (3)
\end{aligned}$$

The spin current $J_{i;j}^S$ for the z-component is expressed in terms of $S_i^\pm = S_i^x \pm iS_i^y$, $J' = \sqrt{J^2+D^2}$, and $\tan\phi_{i;j} = D_{i;j}/J$. While the spin current operator above is well known, the energy current $J_{i;j}^E$ is new. In the Heisenberg limit ($D = 0$) the energy current is directly related to the spin chirality,

$$J_{i;j}^E = J^2\sum_{k\in j}\mathbf{S}_i\cdot(\mathbf{S}_j\times\mathbf{S}_k) \quad (D=0). \quad (4)$$

Linear response theory for the average of spin and energy current operators can be developed now.

Coupling of the energy density H_i to the pseudo-gravitational potential ψ_i is an effective way to derive the thermal response function.[6–8,17] In brief, the total Hamiltonian including the gravitational coupling $H = \sum_i[1+\psi_i e^{st}]H_i$ leads to the modification of the density matrix $\rho(t) = \rho_0 + \delta\rho\, e^{st}$,[17]

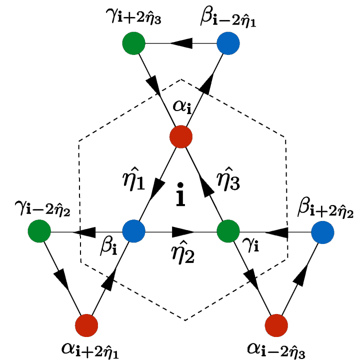

FIG. 1. (Color online) Schematic figure of the Kagome lattice. Arrows indicate the sign convention $D_{i;j} = +D$ for $i \to j$. Unit vectors are chosen $\hat\eta_1 = -(1,\sqrt{3})/2$, $\hat\eta_2 = (1,0)$, $\hat\eta_3 = (-1,\sqrt{3})/2$ with lattice constant $a = 1$. Each upward triangle $\mathbf{i}$ has three sublattice sites $\alpha_{\mathbf{i}}, \beta_{\mathbf{i}}, \gamma_{\mathbf{i}}$.

$$\begin{aligned}
\delta\rho &= -\frac{\rho_0}{\hbar}\int_0^\infty dt' e^{-st'}\int_0^\beta d\beta' \sum_{\langle i,j\rangle}(\psi_j - \psi_i)J_{i;j}^E(-t'-i\beta')\\
&\simeq -\frac{\rho_0}{\hbar}\int_0^\infty dt' e^{-st'}\int_0^\beta d\beta' \sum_{\triangle_{\mathbf{i}}}(\boldsymbol{\nabla}\psi)\cdot\mathbf{j}_0^E(\mathbf{i}; -t'-i\beta').
\end{aligned} \quad (5)$$

The first line involves the sum over all nearest neighbors $\langle i,j\rangle$ of the Kagome lattice, which in the second line is re-organized as a sum over each upward-pointing triangle $\triangle_{\mathbf{i}}$. Assuming smoothly varying field allows one to replace $\psi_j - \psi_i$ by its gradient. The ensuing current vector $\mathbf{j}_0^E(\mathbf{i})$ per triangle $\mathbf{i}$ is a sum,

$$\begin{aligned}
j_{0x}^E(\mathbf{i}) &= J_{\beta_\mathbf{i};\gamma_\mathbf{i}}^E + J_{\gamma_{\mathbf{i}-2\hat\eta_2};\beta_\mathbf{i}}^E\\
&\quad + \frac{1}{2}\Big(J_{\beta_\mathbf{i};\alpha_\mathbf{i}}^E + J_{\alpha_\mathbf{i};\beta_{\mathbf{i}-2\hat\eta_1}}^E + J_{\alpha_\mathbf{i};\gamma_\mathbf{i}}^E + J_{\gamma_\mathbf{i};\alpha_{\mathbf{i}-2\hat\eta_3}}^E\Big),\\
j_{0y}^E(\mathbf{i}) &= \frac{\sqrt{3}}{2}\Big(J_{\beta_\mathbf{i};\alpha_\mathbf{i}}^E + J_{\gamma_\mathbf{i};\alpha_\mathbf{i}}^E + J_{\alpha_\mathbf{i};\gamma_{\mathbf{i}+2\hat\eta_3}}^E + J_{\alpha_\mathbf{i};\beta_{\mathbf{i}-2\hat\eta_1}}^E\Big), \quad (6)
\end{aligned}$$

where all the subscript symbols are as defined in Fig. 1.

As noted long ago by Luttinger,[17] the pseudo-gravitational field entering in the total Hamiltonian alters more than the density matrix, as is often the assumption in linear response theory. Working through the continuity equation for the modified local Hamiltonian $(1+\psi_i)H_i$ gives the new bond energy current operator

$$(1+\psi_i+\psi_j)J_{i;j}^E \simeq [1 + 2(\mathbf{r}_\mathbf{i}\cdot\boldsymbol{\nabla}\psi)]J_{i;j}^E. \quad (7)$$

The failure of the local Hamiltonians to commute with each other, $[H_i, H_j] \neq 0$, is the source of the modification. Such modification does not occur for instance in the case of electric current, since density operators (which couple to electric potential) commute at different sites. The

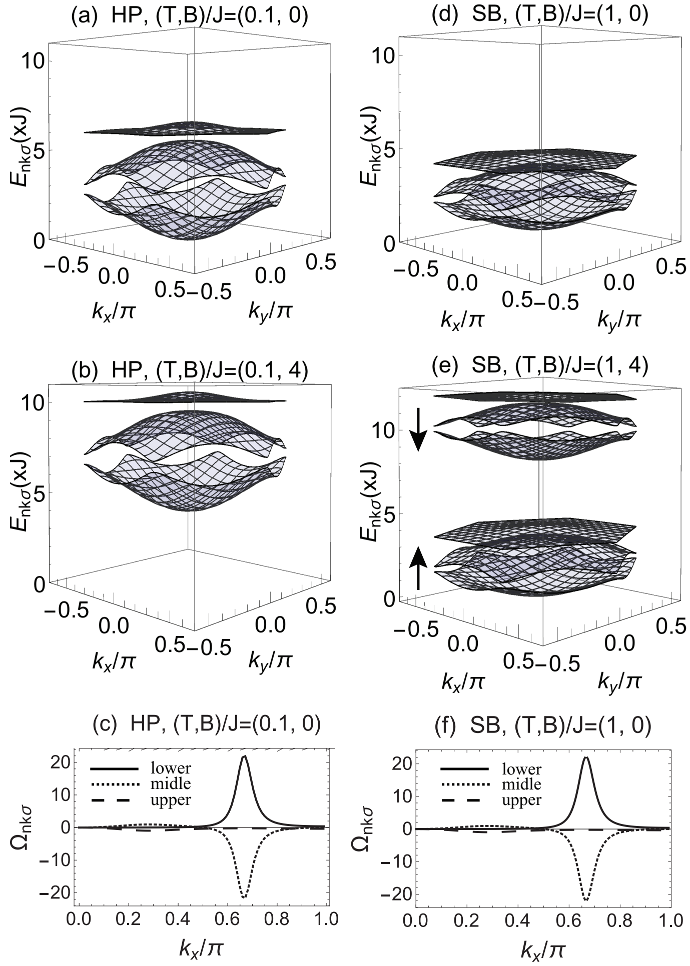

FIG. 2. Magnon band structure from HP theory $(D/J = 0.125)$ at (a) zero and (b) large Zeeman fields. SB band structure for $D/J = 0.125$ at (d) zero and (e) large Zeeman fields. Berry curvatures are worked out at $k_y = 0$ for (c) magnon bands and (f) SB bands of up spins. Hall responses are a consequence of population of low-lying magnon or Schwinger boson bands, multiplied by their respective Berry curvature densities in momentum space. Down-spin SB bands have exactly opposite Berry curvatures at $B = 0$ and a similar one throughout $B > 0$.

relation $\psi_i = \mathbf{r_i} \cdot (\boldsymbol{\nabla}\psi)$ for the uniform potential gradient is assumed. The physical energy current operator is therefore the sum,

$$\begin{aligned}\mathbf{j}^E(\mathbf{i}) &= \mathbf{j}_0^E(\mathbf{i}) + \mathbf{j}_1^E(\mathbf{i}),\\ \mathbf{j}_1^E(\mathbf{i}) &= 2\mathbf{j}_0^E(\mathbf{i})(\mathbf{r_i}\cdot\boldsymbol{\nabla}\psi).\end{aligned} \tag{8}$$

Average of the energy current operator in response to the pseudo-gravitational field accordingly contains two contributions,

$$\langle j_a^E\rangle = \mathrm{Tr}[\delta\rho\, j_{0a}^E] + \mathrm{Tr}[\rho_0\, j_{1a}^E] = (\sigma_{0ab}^E + \sigma_{1ab}^E)(-\boldsymbol{\nabla}_b\psi). \tag{9}$$

Spatial average $(1/N_t)\sum_{\triangle_\mathbf{i}} \mathbf{j}_0^E(\mathbf{i}) \equiv \mathbf{j}^E$, N_t=number of up triangles, is taken. Formal expressions of these coefficients are well-known and reproduced,

$$\begin{aligned}\sigma_{0ab}^E &= \frac{i}{N_t}\sum_{n,m}\frac{e^{-\beta\varepsilon_m} - e^{-\beta\varepsilon_n}}{\varepsilon_m - \varepsilon_n}\frac{\langle n|j_{0b}^E|m\rangle\langle m|j_{0a}^E|n\rangle}{\varepsilon_n - \varepsilon_m - is},\\ \sigma_{1ab}^E &= \mathrm{Tr}\left(\rho_0\left[\frac{\partial j_{0a}^E(\mathbf{q})}{\partial q_b}\right]_{\mathbf{q}=0}\right),\end{aligned} \tag{10}$$

where complete sets of many-body states are $|m\rangle$ and $|n\rangle$ and $\mathbf{j}_0^E(\mathbf{q}) = (1/N_t)\sum_{\triangle_\mathbf{i}} \mathbf{j}_0^E(\mathbf{i})e^{-i\mathbf{q}\cdot\mathbf{r_i}}$.

This completes the derivation of thermal response functions in the spin language. To evaluate them, however, is hard without a full knowledge of all many-body eigenstates for the spin Hamiltonian. Below we propose a scheme in which evaluation of $\sigma_{ab}^E = \sigma_{0ab}^E + \sigma_{1ab}^E$ can be performed straightforwardly at the non-interacting level.

III. HOLSTEIN-PRIMAKOFF AND SCHWINGER BOSON LINEAR RESPONSE THEORY

Evaluation of the response coefficients can be done in the Schwinger boson mean-field theory (SBMFT) in which spin is expressed by a pair of bosons $(b_{i\uparrow}, b_{i\downarrow})$ as $\mathbf{S}_i = \frac{1}{2}\sum_{\alpha,\beta=\uparrow,\downarrow} b_{i\alpha}^\dagger \boldsymbol{\sigma}_{\alpha\beta} b_{i\beta}$. Decoupling in terms of the bond operator $\hat{\chi}_{i;j}^\sigma = b_{i\sigma}^\dagger b_{j\sigma}$ gives the mean-field Hamiltonian,

$$\begin{aligned}H^{\mathrm{SB}} &= \sum_{i,\sigma}(\lambda - \sigma B)b_{i\sigma}^\dagger b_{i\sigma} - \sum_{\langle i,j\rangle,\sigma}\left(t_{i;j}^\sigma b_{i\sigma}^\dagger b_{j\sigma} + h.c.\right),\\ t_{i;j}^\sigma &= J\langle\hat{\chi}_{j;i}^\sigma\rangle + J' e^{-i\sigma\phi_{i;j}}\langle\hat{\chi}_{j;i}^{-\sigma}\rangle.\end{aligned} \tag{11}$$

The Lagrange multipler λ is introduced to keep the average boson number constant at $2S = 1$. The Zeeman field and the effective flux from DM interaction act oppositely for the two bosons. The energy current operator in Eq. (3) allows a lengthy re-writing in terms of bond operators

$$J^E_{i;j} = -\frac{1}{2}B(J+iD_{i;j})\sum_\sigma \hat\chi^{-\sigma}_{i;j}\hat\chi^{\sigma}_{j;i} + \frac{1}{16i}\sum_{k\in j}\Bigg\{J^2(\hat\chi_{i;j}\hat\chi_{j;k}\hat\chi_{k;i} - h.c.) + D_{i;j}D_{j;k}\sum_\sigma\left(\hat\chi^{-\sigma}_{i;j}\hat\chi^{-\sigma}_{j;k}\hat\chi^{\sigma}_{k;i} - h.c.\right)$$
$$+iJ\sum_\sigma \sigma\left(D_{i;j}\hat\chi^{-\sigma}_{i;j}\hat\chi_{j;k}\hat\chi^{\sigma}_{k;i} + D_{j;k}\hat\chi^{-\sigma}_{k;j}\hat\chi_{j;i}\hat\chi^{\sigma}_{i;k} + h.c.\right)\Bigg\} - (i\leftrightarrow j), \quad (12)$$

where $\hat\chi_{i;j} = \sum_\sigma \hat\chi^\sigma_{i;j}$, and $(i\leftrightarrow j)$ denotes the exchange for all the terms shown in Eq. (12).

Due to the enormous complexity of the current operator in the Schwinger boson representation (or in the spin representation for that matter), calculating the correlation function for it appears daunting if not impossible. However, one observes that each triple product of bond operators in the above expression contains exactly two terms that can be replaced by the mean-field average $\langle\hat\chi^\sigma_{i;j}\rangle$ (because they span the nearest neighbours in the Kagome lattice), and only one that contains boson hopping across second neighbors (not captured by the mean-field parameterization). After such mean-field reduction $J^E_{i;j}$ becomes a bilinear in the Schwinger boson operator [see Appendix A]. In the uniform case, $\langle\hat\chi^\sigma_{i;j}\rangle = \chi_\sigma$, we have proven that the corresponding mean-field vector current operator $\mathbf{j}^E_0(\mathbf{i})$, averaged over all triangles $\mathbf{j}^E_0 = (1/N_t)\sum_{\triangle_\mathbf{i}}\mathbf{j}^E_0(\mathbf{i})$, is equal to a simple and familiar expression [see Appendix A]

$$\mathbf{j}^E_0 = \frac{1}{2}\sum_{\mathbf{k},\sigma}\Psi^\dagger_{\mathbf{k}\sigma}\left(H^{\rm SB}_{\mathbf{k}\sigma}\frac{\partial H^{\rm SB}_{\mathbf{k}\sigma}}{\partial\mathbf{k}} + \frac{\partial H^{\rm SB}_{\mathbf{k}\sigma}}{\partial\mathbf{k}}H^{\rm SB}_{\mathbf{k}\sigma}\right)\Psi_{\mathbf{k}\sigma}. \quad (13)$$

We denote the three corners of the upward triangle $\mathbf{i}$ as $\alpha_\mathbf{i},\beta_\mathbf{i},\gamma_\mathbf{i}$, respectively (Fig. 1), and their Fourier counterparts as $\Psi^T_{\mathbf{k}\sigma} = (\alpha_{\mathbf{k}\sigma}\ \beta_{\mathbf{k}\sigma}\ \gamma_{\mathbf{k}\sigma})$. Mean-field SB Hamiltonian in Eq. (11) for uniform parameters becomes in momentum space $H^{\rm SB} = \sum_{\mathbf{k},\sigma}\Psi^\dagger_{\mathbf{k}\sigma}H^{\rm SB}_{\mathbf{k}\sigma}\Psi_{\mathbf{k}\sigma}$,

$$H^{\rm SB}_{\mathbf{k}\sigma} = (\lambda-\sigma B)I_3 + \begin{pmatrix} 0 & t_\sigma\cos k_1 & t^*_\sigma\cos k_3 \\ t^*_\sigma\cos k_1 & 0 & t_\sigma\cos k_2 \\ t_\sigma\cos k_3 & t^*_\sigma\cos k_2 & 0\end{pmatrix}, \quad (14)$$

with effective hopping parameters $t_\sigma = J\chi - i\sigma D\chi_{-\sigma}$, $\chi = \sum_\sigma\chi_\sigma$, $k_x = \mathbf{k}\cdot\hat\eta_x$ and $\hat\eta_x$ are the three orientation unit vectors defined in Fig. 1. We note that for each spin σ, both the current operator $\mathbf{j}^E_{\mathbf{k}\sigma}$ and the Hamiltonian $H_{\mathbf{k}\sigma}$ have identical forms as those already examined for magnon thermal Hall problem on the Kagome lattice. [4,8] Thus, known thermal Hall formulas derived previously can be applied here directly, for evaluation *in the paramagnetic regime.*

The thermal Hall conductivity within the SB theory reads

$$\kappa^{\rm SB}_{xy} = -\frac{k_B^2T}{\hbar N_t}\sum_{\mathbf{k},n,\sigma}\left[c_2\left(E^{\rm SB}_{n\mathbf{k}\sigma}\right) - \frac{\pi^2}{3}\right]\Omega^{\rm SB}_{n\mathbf{k}\sigma}. \quad (15)$$

Both the energy dispersions and Berry curvatures are to be obtained from diagonalizing the Hamiltonian, Eq. (14), $c_2(x) = (1+x)\left(\ln\frac{1+x}{x}\right)^2 - (\ln x)^2 - 2\mathrm{Li}_2(-x)$, [8] and $\Omega^{\rm SB}_{n\mathbf{k}\sigma} = i\langle\partial_{k_x}u_{n\mathbf{k}\sigma}|\partial_{k_y}u_{n\mathbf{k}\sigma}\rangle + c.c.$ for the n-th band eigenstate $|u_{n\mathbf{k}\sigma}\rangle$ of $H^{\rm SB}_{\mathbf{k}\sigma}$.

By comparison, HP substitution of spin operators in the spin Hamiltonian (1) leads to the familiar magnon Hamiltonian [4]

$$H^{\rm HP} = -SJ'\sum_{\langle i,j\rangle}(e^{-i\phi_{i,j}}b^\dagger_ib_j + h.c.) + \sum_i(B+4SJ)b^\dagger_ib_i,$$

where S is the size of average magnetization, either by spontaneous order or through external field. Different from earlier work [4] we invoke self-consistency relation

$$S(B,T) = \frac{1}{2}\tanh\left[\frac{B+4JS(B,T)}{2k_BT}\right]$$

to work out S at a given temperature and field strength. Spontaneous magnetization $S\neq 0$ occurs at $T^{\rm HP}_c = J$. Magnon thermal Hall formula $\kappa^{\rm HP}_{xy}$ is obtained the same way as in Eq. (15) without the sum over the spin index σ.

Figure 2 shows representative band dispersions and Berry curvature distributions over the first Brillouin zone for SB and HP bosons, respectively. At $B=0$ both SB bands look nearly identical to the magnon bands except for the non-zero band minimum (SB bosons are not Goldstone bosons). The zero-field Berry curvatures are also quite similar for SB and HP bosons, as shown in Fig. 2, but not identical, because effective DM constant in the SB theory is halved, $t_\sigma = J\chi - i\sigma\chi_{-\sigma} = \chi(J-\sigma D/2)$, at $B=0$.

Figure 3 displays thermal Hall response coefficients from HP and SB theories. Recall that $\kappa^{\rm HP}_{xy}$ is finite even at zero field, due to the spontaneous flux generated by the DM interaction. [4] The $B=0$ value however changes sign upon raising the temperature as shown in Fig. 3(a), because the higher magnon band has the opposite Berry curvature as shown in Fig. 2(c). On further increase of T it goes down to zero at $T = T^{\rm HP}_c$. There is also a sign reversal of the Hall response at finite field, in qualitative agreement with the recent measurement reported by the Ong group [13]. At low temperature and low field the lowest-lying magnon band dominates transport. For higher temperatures, higher-energy band carrying opposite Berry flux (see Fig. 2(c)) has a chance to contribute

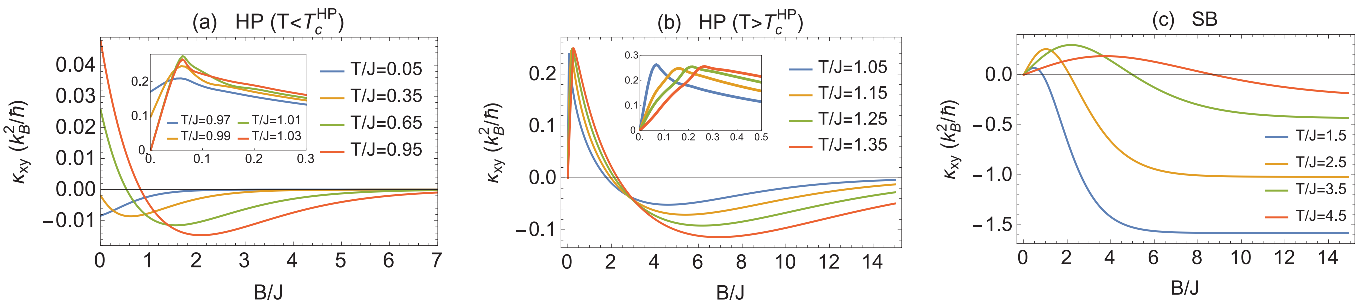

FIG. 3. (Color online) Low-temperature thermal Hall conductivity based on self-consistent HP theory ($D/J = 0.125$) for (a) $T < T_c^{\mathrm{HP}}$ and (b) $T > T_c^{\mathrm{HP}}$. Zero-field ferromagnetic transition occurs at $T_c^{\mathrm{HP}}/J = 1$. Inset to (a) highlights the sensitive dependence of $\kappa_{xy}^{\mathrm{HP}}$ on temperature around $T = T_c^{\mathrm{HP}}$ due to small values of self-consistent magnetization S and the consequent collapse of magnon bands, leading to a large enhancement of the Bose factor in Eq. (15) over a small temperature change. Inset to (b) emphasizes the linear rise of $\kappa_{xy}^{\mathrm{HP}}$ with magnetic field for $T > T_c^{\mathrm{HP}}$. (c) High-temperature thermal Hall conductivity based on SBMFT ($D/J = 0.15$) for $T > T_c^{\mathrm{SB}}(\approx 0.5J)$.

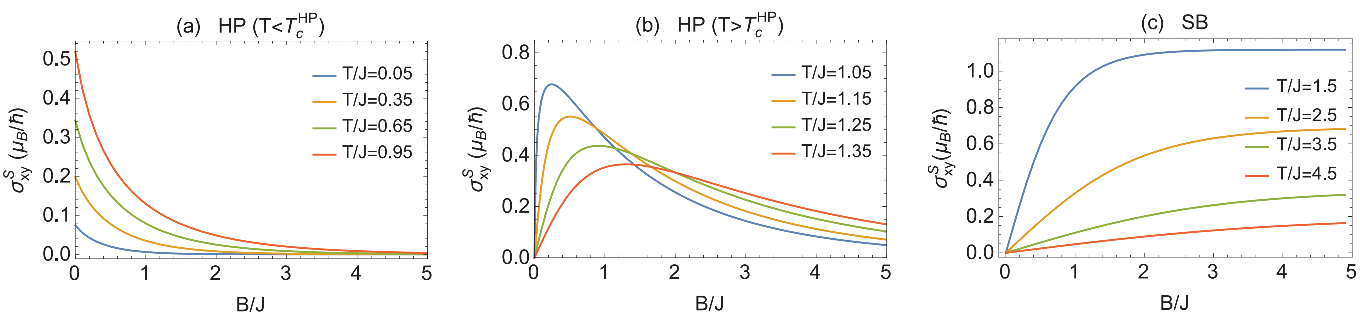

FIG. 4. (Color online) Spin Hall conductivity σ_{xy}^S based on HP theory ($D/J = 0.125$) for (a) $T < T_c^{\mathrm{HP}}$ and (b) $T > T_c^{\mathrm{HP}}$. (c) High-temperature spin Hall conductivity based on SBMFT ($D/J = 0.15$) for $T > T_c^{\mathrm{SB}}$.

significantly. Strong Zeeman field creates a large gap for all the bands, diminishing the thermal population difference among the bands and increasing the relative contribution of the higher band with significant Berry flux concentration. The Schwinger boson Hall transport, shown in Fig. 3(c), is already at quite high a temperature and continues the trend seen in the high-temperature magnon calculation, i.e. a positive peak at low field followed by a long negative tail in the high-field region. Together, we are assured that thermal Hall transport is a sensitive probe of the Berry flux distribution as well as the band structure of the underlying elementary excitations in an insulating paramagnet.

The spin Hall response can be worked out in much the same way by replacing the spin current operator in Eq. (3) with its mean-field version [see Appendix B]. The source term for spin current, $-\sum_i h_i S_i^z$, does not modify the spin continuity equation since $[S_i^z, S_j^z] = 0$. Mean-field spin current operator

$$\mathbf{j}^S = \sum_{\mathbf{k},\sigma} \sigma \Psi_{\mathbf{k}\sigma}^\dagger \frac{\partial H_{\mathbf{k}\sigma}}{\partial \mathbf{k}} \Psi_{\mathbf{k}\sigma}$$

results in the spin Hall conductivity

$$\sigma_{xy}^{S,\mathrm{SB}} = \frac{\mu_B}{\hbar N_t} \sum_{\mathbf{k},n,\sigma} n_B(E_{n\mathbf{k}\sigma}) \Omega_{\mathbf{k},n,\sigma}^{\mathrm{SB}}, \qquad (16)$$

where n_B is the Bose occupation function. Spin Hall coefficients for both HP and SB boson theories are worked out in Fig. 4.

IV. DISCUSSION

Theories of thermal and spin Hall effects for spin systems are developed in the general language of spin operators. Ways to consistently obtain response functions in the correlated disordered phase are developed, employing Schwinger boson approach. The Holstein-Primakoff reduction is shown to reproduce the existing theories. Most interestingly, Eq. (4) unambiguously points out that thermal Hall response is a direct measure of the inherent spin chirality in the underlying system, along with other spectroscopic probes of spin chirality recently proposed [18,19]. As our derivations in Sec. II do not assume a particular lattice geometry, the formalisms developed in this paper will be applicable to spin models defined on any lattice geometry in both two and three dimensions.

Regarding the actual computation of the thermal and spin Hall response functions we have employed self-consistent Holstein-Primakoff and Schwinger boson methods in this paper. Other means of computing the thermal Hall coefficients in the spin system, such as exact diagonalization, can be an alternative to the methods presented in this paper. There are shortcomings in the so-called "exact methods" due to the severe size limitations in the diagonalization and the difficulty of extrapolating the computation to large system size. The abundance of low-energy states that are crucial to efficient thermal transport may be difficult to capture in the exact diagonalization on small system size. On the other hand, the mean-field nature in the Schwinger boson approach calls for improvements in regard to effects of fluctuations[15,16,20]. In particular the phase fluctuation in the mean-field order parameter $t^{\sigma}_{i;j}$ may remain gapless and severely disrupt the mean-field analysis unless well-known mass-generating mechanisms (such as Anderson-Higgs or Chern-Simons) play a role. We plan to complement the present work, focused on the formulation of spin thermal transport and its evaluation in the simplest possible manner, in several directions with the forthcoming publication with emphasis on the importance of gauge fluctuations in the Schwinger boson formalism.

ACKNOWLEDGMENTS

J. H. H. is supported by the NRF grant (No. 2013R1A2A1A01006430) and wishes to acknowledge the hospitality of the condensed matter theory group at MIT and Boston College where this work was carried out. P.A.L. acknowledges support by the DOE grant DE-FG01-03-ER46076. We are grateful to Robin Chisnell, Young S. Lee, and Phuan Ong for many inspiring discussions.

---

* Electronic address: hanjh@skku.edu

† Electronic address: palee@mit.edu

1 N. Nagaosa, J. Sinova, S. Onoda, A. H. MacDonald, and N. P. Ong, Rev. Mod. Phys. **82**, 1539 (2010), URL `http://link.aps.org/doi/10.1103/RevModPhys.82.1539`.

2 D. Xiao, M.-C. Chang, and Q. Niu, Rev. Mod. Phys. **82**, 1959 (2010), URL `http://link.aps.org/doi/10.1103/RevModPhys.82.1959`.

3 C. Strohm, G. L. J. A. Rikken, and P. Wyder, Phys. Rev. Lett. **95**, 155901 (2005), URL `http://link.aps.org/doi/10.1103/PhysRevLett.95.155901`.

4 H. Katsura, N. Nagaosa, and P. A. Lee, Phys. Rev. Lett. **104**, 066403 (2010), URL `http://link.aps.org/doi/10.1103/PhysRevLett.104.066403`.

5 Y. Onose, T. Ideue, H. Katsura, Y. Shiomi, N. Nagaosa, and Y. Tokura, Science **329**, 297 (2010), http://www.sciencemag.org/content/329/5989/297.full.pdf, URL `http://www.sciencemag.org/content/329/5989/297.abstract`.

6 R. Matsumoto and S. Murakami, Phys. Rev. Lett. **106**, 197202 (2011), URL `http://link.aps.org/doi/10.1103/PhysRevLett.106.197202`.

7 R. Matsumoto and S. Murakami, Phys. Rev. B **84**, 184406 (2011), URL `http://link.aps.org/doi/10.1103/PhysRevB.84.184406`.

8 R. Matsumoto, R. Shindou, and S. Murakami, Phys. Rev. B **89**, 054420 (2014), URL `http://link.aps.org/doi/10.1103/PhysRevB.89.054420`.

9 L. Zhang, J. Ren, J.-S. Wang, and B. Li, Phys. Rev. B **87**, 144101 (2013), URL `http://link.aps.org/doi/10.1103/PhysRevB.87.144101`.

10 A. Mook, J. Henk, and I. Mertig, Phys. Rev. B **89**, 134409 (2014), URL `http://link.aps.org/doi/10.1103/PhysRevB.89.134409`.

11 V. Kalmeyer and R. B. Laughlin, Phys. Rev. Lett. **59**, 2095 (1987), URL `http://link.aps.org/doi/10.1103/PhysRevLett.59.2095`.

12 X. G. Wen, F. Wilczek, and A. Zee, Phys. Rev. B **39**, 11413 (1989), URL `http://link.aps.org/doi/10.1103/PhysRevB.39.11413`.

13 M. Hirschberger, R. Chisnell, Y. S. Lee, and N. P. Ong, arXiv:1502.05688.

14 M. Hirschberger, R. J. Krizan, Jason W. Cava, and N. P. Ong, arXiv:1502.02006v1.

15 D. P. Arovas and A. Auerbach, Phys. Rev. B **38**, 316 (1988), URL `http://link.aps.org/doi/10.1103/PhysRevB.38.316`.

16 A. Auerbach, *Interacting Electrons and Quantum Magnetism*, Graduate Texts in Contemporary Physics (Springer New York, 1994), ISBN 9780387942865, URL `https://books.google.com/books?id=tiQlKzJa6GEC`.

17 J. M. Luttinger, Phys. Rev. **135**, A1505 (1964), URL `http://link.aps.org/doi/10.1103/PhysRev.135.A1505`.

18 W.-H. Ko and P. A. Lee, Phys. Rev. B **84**, 125102 (2011), URL `http://link.aps.org/doi/10.1103/PhysRevB.84.125102`.

19 P. A. Lee and N. Nagaosa, Phys. Rev. B **87**, 064423 (2013), URL `http://link.aps.org/doi/10.1103/PhysRevB.87.064423`.

20 S. Sachdev, Phys. Rev. B **45**, 12377 (1992), URL `http://link.aps.org/doi/10.1103/PhysRevB.45.12377`.

Appendix A: Energy current operator in the Schwinger boson mean field theory

The bond energy current operator appearing in the continuity equation $\dot{H}_i + \sum_j J^E_{i;j} = 0$ was written in terms of Schwinger boson operator in the following way,

$$
\begin{aligned}
J^E_{i;j} &= -\frac{1}{2}B(J+iD_{i;j})\sum_\sigma \hat{\chi}^{-\sigma}_{i;j}\hat{\chi}^{\sigma}_{j;i} \\
&+ \frac{1}{16i}\sum_{k\in j}\Bigg\{J^2\left[\hat{\chi}_{i;j}\hat{\chi}_{j;k}\hat{\chi}_{k;i} - h.c.\right] + D_{i;j}D_{j;k}\sum_\sigma\left[\hat{\chi}^{-\sigma}_{i;j}\hat{\chi}^{-\sigma}_{j;k}\hat{\chi}^{\sigma}_{k;i} - h.c.\right] \\
&+ iJ\sum_\sigma \sigma\left(D_{i;j}\hat{\chi}^{-\sigma}_{i;j}\hat{\chi}_{j;k}\hat{\chi}^{\sigma}_{k;i} + D_{j;k}\hat{\chi}^{-\sigma}_{k;j}\hat{\chi}_{j;i}\hat{\chi}^{\sigma}_{i;k} + h.c.\right)\Bigg\} - (i\leftrightarrow j). \qquad \text{(A1)}
\end{aligned}
$$

This expression has six boson operators multiplied together and it is impractical to carry out linear response calculations for it. On implementing the mean field substitution for the nearest-neighbor bond operators $\langle\hat{\chi}^{\sigma}_{i;j}\rangle = \langle b^\dagger_{i\sigma}b_{j\sigma}\rangle \equiv \chi_\sigma$ or χ^*_σ following the same convention as for DM interaction depicted in Fig. 1 of the main text, we obtain the mean-field energy current operator

$$
\begin{aligned}
J^E_{i;j} &\overset{\text{SBMF}}{\longrightarrow} -\frac{1}{4}B(J+iD_{i;j})\sum_\sigma\left[\langle\hat{\chi}^{-\sigma}_{i;j}\rangle\hat{\chi}^{\sigma}_{j;i} + \hat{\chi}^{-\sigma}_{i;j}\langle\hat{\chi}^{\sigma}_{j;i}\rangle\right] \\
&+ \frac{1}{16i}\sum_{k\in j}\Bigg\{J^2\left[\langle\hat{\chi}_{i;j}\rangle\langle\hat{\chi}_{j;k}\rangle\hat{\chi}_{k;i} - h.c.\right] + D_{i;j}D_{j;k}\sum_\sigma\left(\langle\hat{\chi}^{-\sigma}_{i;j}\rangle\langle\hat{\chi}^{-\sigma}_{j;k}\rangle\hat{\chi}^{\sigma}_{k;i} - h.c.\right) \\
&+ iJ\sum_\sigma\sigma\left(D_{i;j}\langle\hat{\chi}^{-\sigma}_{i;j}\rangle\langle\hat{\chi}_{j;k}\rangle\hat{\chi}^{\sigma}_{k;i} + D_{j;k}\langle\hat{\chi}^{-\sigma}_{k;j}\rangle\langle\hat{\chi}_{j;i}\rangle\hat{\chi}^{\sigma}_{i;k} + h.c.\right)\Bigg\} - (i\leftrightarrow j). \qquad \text{(A2)}
\end{aligned}
$$

Only the bond operators connecting second-nearest neighbors remain as operators now. It is a boson bi-linear. Here the MF parameter substitution needs to be done carefully, because it could be either χ_σ or χ^*_σ depending i and j as explained before. Using the above expression and Eq. 5 of the main text (reproduced here)

$$
\begin{aligned}
j^E_{0x}(\mathbf{i}) &= J^E_{\beta_\mathbf{i};\gamma_\mathbf{i}} + J^E_{\gamma_{\mathbf{i}-2\hat{\eta}_2};\beta_\mathbf{i}} + \frac{1}{2}\Big(J^E_{\beta_\mathbf{i};\alpha_\mathbf{i}} + J^E_{\alpha_\mathbf{i};\beta_{\mathbf{i}-2\hat{\eta}_1}} + J^E_{\alpha_\mathbf{i};\gamma_\mathbf{i}} + J^E_{\gamma_\mathbf{i};\alpha_{\mathbf{i}-2\hat{\eta}_3}}\Big), \\
j^E_{0y}(\mathbf{i}) &= \frac{\sqrt{3}}{2}\Big(J^E_{\beta_\mathbf{i};\alpha_\mathbf{i}} + J^E_{\gamma_\mathbf{i};\alpha_\mathbf{i}} + J^E_{\alpha_\mathbf{i};\gamma_{\mathbf{i}+2\hat{\eta}_3}} + J^E_{\alpha_\mathbf{i};\beta_{i-2\hat{\eta}_1}}\Big), \qquad \text{(A3)}
\end{aligned}
$$

one can convert the bond current to the vector current operator $j^E_{0x}(\mathbf{i})$ and $j^E_{0y}(\mathbf{i})$. Note that each bond current operator $J^E_{i;j}$ itself consists of dozen different terms as shown in Eq. (3) of the main article. Each vector current operator then consists of $\sim 10^2$ terms. Assignment of χ_σ or χ^*_σ for each average in the above equation (2) has to be carried out out term-by-term. Having completed such exercise, we finally arrive at the momentum-space expression for the current operator,

$$
j^E_{0\alpha} = \frac{1}{N_t}\sum_{\triangle_\mathbf{i}} j^E_{0\alpha}(\mathbf{i}) = \sum_{\mathbf{k},\sigma}\Psi^\dagger_{\mathbf{k}\sigma}\left(J^2\mathcal{A}_{\alpha\mathbf{k}} + JD\,\mathcal{B}_{\alpha\mathbf{k}\sigma} + D^2\mathcal{C}_{\alpha\mathbf{k}\sigma}\right)\Psi_{\mathbf{k}\sigma}, \qquad \text{(A4)}
$$

where for the $x-$direction

$$
\mathcal{A}_{x\mathbf{k}} = \begin{pmatrix}
\frac{|\chi|^2}{2}[\sin 2k_1 + \sin 2k_3] & -\frac{(\chi^*)^2}{4}[3\sin(k_2-k_3)+\sin(k_2+k_3)] & \frac{\chi^2}{4}[3\sin(k_2-k_1)+\sin(k_2+k_1)] \\
-\frac{\chi^2}{4}[3\sin(k_2-k_3)+\sin(k_2+k_3)] & \frac{|\chi|^2}{2}[\sin 2k_1 - 2\sin 2k_2] & \frac{(\chi^*)^2}{2}\sin(k_1+k_3) \\
\frac{(\chi^*)^2}{4}[3\sin(k_2-k_1)+\sin(k_2+k_1)] & \frac{\chi^2}{2}\sin(k_1+k_3) & \frac{|\chi|^2}{2}[\sin 2k_3 - 2\sin 2k_2]
\end{pmatrix},
$$

$$
\mathcal{B}_{x\mathbf{k}\sigma} = \sigma\begin{pmatrix}
\mathrm{Im}[\chi\,\chi^*_{-\sigma}](\sin 2k_1+\sin 2k_3) & i(\chi\,\chi_{-\sigma})^*[\sin(k_3+k_2)-3\sin(k_3-k_2)] & i\chi\,\chi_{-\sigma}[\sin(k_2+k_1)-3\sin(k_2-k_1)] \\
-i\chi\,\chi_{-\sigma}[\sin(k_3+k_2)-3\sin(k_3-k_2)] & \mathrm{Im}[\chi\,\chi_{-\sigma}](\sin 2k_1 - 2\sin 2k_2) & -i(\chi\,\chi_{-\sigma})^*\sin(k_1+k_3) \\
-i(\chi\,\chi_{-\sigma})^*[\sin(k_2+k_1)-3\sin(k_2-k_1)] & i\chi\,\chi_{-\sigma}\sin(k_1+k_3) & \mathrm{Im}[\chi\,\chi_{-\sigma}](\sin 2k_3 - 2\sin 2k_2)
\end{pmatrix},
$$

$$
\mathcal{C}_{x\mathbf{k}\sigma} = \begin{pmatrix}
\frac{|\chi|^2}{2}[\sin 2k_1+\sin 2k_3] & \frac{(\chi^*_{-\sigma})^2}{4}[3\sin(k_2-k_3)+\sin(k_2+k_3)] & -\frac{\chi^2_{-\sigma}}{4}[3\sin(k_2-k_1)+\sin(k_2+k_1)] \\
\frac{\chi^2_{-\sigma}}{4}[3\sin(k_2-k_3)+\sin(k_2+k_3)] & \frac{|\chi|^2}{2}[\sin 2k_1 - 2\sin 2k_2] & -\frac{(\chi^*_{-\sigma})^2}{2}\sin(k_1+k_3) \\
-\frac{(\chi^*_{-\sigma})^2}{4}[3\sin(k_2-k_1)+\sin(k_2+k_1)] & -\frac{\chi^2_{-\sigma}}{2}\sin(k_1+k_3) & \frac{|\chi|^2}{2}[\sin 2k_3 - 2\sin 2k_2]
\end{pmatrix},
$$

and for y-direction,

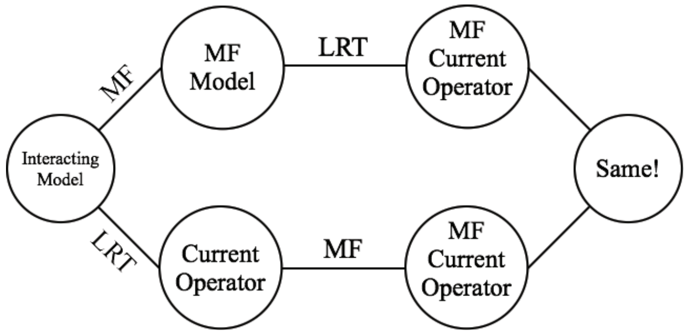

FIG. 5. Schematic figure demonstrating the equivalence we have provided in Appendix A. MF (mean field) and LRT (linear response theory) procedures can be interchanged, leading to the same, final linear response coefficients.

$$
\mathcal{A}_{y\mathbf{k}} = \sqrt{3}\begin{pmatrix} \frac{|\chi|^2}{2}\left[\sin 2k_1 - \sin 2k_3\right] & -\frac{(\chi^*)^2}{4}\cos k_2 \sin k_3 & \frac{\chi^2}{4}\cos k_2 \sin k_1 \\ -\frac{\chi^2}{2}\cos k_2 \sin k_3 & \frac{|\chi|^2}{2}\sin 2k_1 & \frac{(\chi^*)^2}{2}\sin(k_1-k_3) \\ \frac{(\chi^*)^2}{4}\cos k_2 \sin k_1 & \frac{\chi^2}{2}\sin(k_1-k_3) & -\frac{|\chi|^2}{2}\sin 2k_3 \end{pmatrix},
$$

$$
\mathcal{B}_{y\mathbf{k}\sigma} = \sigma\sqrt{3}\begin{pmatrix} \mathrm{Im}[\chi\,\chi^*_{-\sigma}]\left[\sin 2k_1 - \sin 2k_3\right] & i(\chi\,\chi_{-\sigma})^*\cos k_2 \sin k_3 & i\chi\,\chi_{-\sigma}\cos k_2 \sin k_1 \\ -i\chi\,\chi_{-\sigma}\cos k_2 \sin k_3 & \mathrm{Im}[\chi\,\chi_{-\sigma}]\sin 2k_1 & -i(\chi\,\chi_{-\sigma})^*\sin(k_1-k_3) \\ -i(\chi\,\chi_{-\sigma})^*\cos k_2 \sin k_1 & i\chi\,\chi_{-\sigma}\sin(k_1-k_3) & \mathrm{Im}[\chi\,\chi_{-\sigma}]\cos k_3 \sin k_3 \end{pmatrix},
$$

$$
\mathcal{C}_{y\mathbf{k}\sigma} = \sqrt{3}\begin{pmatrix} \frac{|\chi|^2}{2}\left[\sin 2k_1 - \sin 2k_3\right] & \frac{(\chi^*_{-\sigma})^2}{4}\cos k_2 \sin k_3 & -\frac{\chi^2_{-\sigma}}{4}\cos k_2 \sin k_1 \\ \frac{\chi^2_{-\sigma}}{4}\cos k_2 \sin k_3 & \frac{|\chi|^2}{2}\sin 2k_1 & -\frac{(\chi^*_{-\sigma})^2}{2}\sin(k_1-k_3) \\ -\frac{(\chi^*_{-\sigma})^2}{4}\cos k_2 \sin k_1 & -\frac{(\chi_{-\sigma})^2}{2}\sin(k_1-k_3) & -\frac{|\chi|^2}{2}\sin 2k_3 \end{pmatrix}.
$$

Remarkably, the hopelessly lengthy expression found above is completely equal, term-by-term, to the following much simpler and intuitive expression

$$
\mathbf{j}_0^E = \frac{1}{2}\sum_{\mathbf{k},\sigma}\Psi^\dagger_{\mathbf{k}\sigma}\left(H_{\mathbf{k}\sigma}\frac{\partial H_{\mathbf{k}\sigma}}{\partial \mathbf{k}} + \frac{\partial H_{\mathbf{k}\sigma}}{\partial \mathbf{k}}H_{\mathbf{k}\sigma}\right)\Psi_{\mathbf{k}\sigma}. \tag{A5}
$$

Here $H_{\mathbf{k}\sigma}$ is the Schwinger boson mean-field Hamiltonian mapping of the original spin Hamiltonian. Reproducing Eq. (10) of the main text,

$$
\begin{aligned}
H^{\mathrm{SB}} &= \sum_{i,\sigma}(\lambda - \sigma B)b^\dagger_{i\sigma}b_{i\sigma} - \sum_{\langle i,j\rangle,\sigma}\left(t^\sigma_{i;j}b^\dagger_{i\sigma}b_{j\sigma} + h.c.\right), \\
t^\sigma_{i;j} &= J\langle\hat{\chi}^\sigma_{j;i}\rangle + J'e^{-i\sigma\phi_{i;j}}\langle\hat{\chi}^{-\sigma}_{j;i}\rangle,
\end{aligned} \tag{A6}
$$

and making proper uniform-state ansatz $\langle\hat{\chi}^\sigma_{i;j}\rangle = \chi_\sigma$ (χ^*_σ) gives the momentum space Schwinger boson Hamiltonian [Eq. (13) of the main article]

$$
H^{\mathrm{SB}}_{\mathbf{k}\sigma} = (\lambda - \sigma B)I_3 + \begin{pmatrix} 0 & t_\sigma\cos k_1 & t^*_\sigma\cos k_3 \\ t^*_\sigma\cos k_1 & 0 & t_\sigma\cos k_2 \\ t_\sigma\cos k_3 & t^*_\sigma\cos k_2 & 0 \end{pmatrix}. \tag{A7}
$$

Meaning of the complete equivalence we just obtained is given schematically in Fig. 1. One starts with an interacting spin model, derive the proper energy current operator from it, and then reduce it to its mean-field form (bottom path of the flow in Fig. 1). On the other hand, one can begin by writing down the mean-field Hamiltonian for the interacting spin model first, and derive the current operator from the mean-field, non-interacting Hamiltonian (top path of the flow). The results, as we demonstrate here, are identical. All the convenient machinery of linear response theory for non-interacting models can be brought to bear on the interacting problem now.

Appendix B: Spin current operator in Schwinger boson mean field theory

As for the spin current operator, we can follow the same procedure developed for dealing with the energy current operator in the previous section. First one converts the bond spin current operator to the vector spin current according to Eq. (3) [Eq. (5) of main text], then take average over the whole lattice. In momentum space we get

$$\begin{aligned} J^S_{i;j} &= -\frac{i}{2}(J + iD_{i;j})S^+_i S^-_j + h.c. \\ &\xrightarrow{\text{MF}} -\frac{1}{4}(J + iD_{i;j})\sum_\sigma \left[\langle \hat{\chi}^{-\sigma}_{i;j}\rangle \hat{\chi}^{\sigma}_{j;i} + \hat{\chi}^{-\sigma}_{i;j}\langle \hat{\chi}^{\sigma}_{j;i}\rangle\right]. \end{aligned}$$

Using Eq. (5) of main article, we can define the spin current operator on the kagome lattice, and then obtain

$$j^S_\alpha = \frac{1}{N_t}\sum_{\triangle_{\mathbf{i}}} j^S_\alpha(\mathbf{i}) = \sum_{\mathbf{k},\sigma}\sigma\Psi^\dagger_{\mathbf{k}\sigma}\mathcal{S}_{\alpha\mathbf{k}\sigma}\Psi_{\mathbf{k}\sigma}, \tag{B1}$$

where

$$\begin{aligned} \mathcal{S}_{x\mathbf{k}\sigma} &= \begin{pmatrix} 0 & \frac{1}{2}\left(J\chi + i\sigma D\chi_{-\sigma}\right)\sin k_1 & \frac{1}{2}(J\chi^* - i\sigma D\chi^*_{-\sigma})\sin k_3 \\ \frac{1}{2}\left(J\chi^* - i\sigma D\chi^*_{-\sigma}\right)\sin k_1 & 0 & (J\chi + i\sigma D\chi_{-\sigma})\sin k_2 \\ \frac{1}{2}\left(J\chi + i\sigma D\chi_{-\sigma}\right)\sin k_3 & (J\chi^* - i\sigma D\chi^*_{-\sigma})\sin k_2 & 0 \end{pmatrix}, \\ \mathcal{S}_{y\mathbf{k}\sigma} &= \begin{pmatrix} 0 & \frac{\sqrt{3}}{2}\left(J\chi + i\sigma D\chi_{-\sigma}\right)\sin k_1 & -\frac{\sqrt{3}}{2}(J\chi^* - i\sigma D\chi^*_{-\sigma})\sin k_3 \\ \frac{\sqrt{3}}{2}\left(J\chi^* - i\sigma D\chi^*_{-\sigma}\right)\sin k_1 & 0 & 0 \\ -\frac{\sqrt{3}}{2}\left(J\chi + i\sigma D\chi_{-\sigma}\right)\sin k_3 & 0 & 0 \end{pmatrix}. \end{aligned}$$

Again, we find complete equivalence of this to the current operator derived from the mean-field Hamiltonian,

$$\mathbf{j}^S = \sum_{\mathbf{k}\sigma}\sigma\Psi^\dagger_{\mathbf{k}\sigma}\frac{\partial H_{\mathbf{k}\sigma}}{\partial\mathbf{k}}\Psi_{\mathbf{k}\sigma}. \tag{B2}$$